IEEE Access
Multidisciplinary ⋮ Rapid Review ⋮ Open Access Journal

Received January 10, 2021, accepted January 28, 2021, date of publication February 2, 2021, date of current version February 9, 2021.

Digital Object Identifier 10.1109/ACCESS.2021.3056281

Power Semiconductor Devices and Packages: Solder Mechanical Characterization and Lifetime Prediction

MICHELE CALABRETTA[1], ALESSANDRO SITTA[1], SALVATORE MASSIMO OLIVERI[2], AND GAETANO SEQUENZIA[2]

[1]Automotive and Discrete Group, Research and Development Department, STMicroelectronics, 95121 Catania, Italy
[2]Dipartimento di Ingegneria Elettrica, Elettronica ed Informatica (DIEEI), Università degli Studi di Catania, 95125 Catania, Italy

Corresponding author: Michele Calabretta (michele.calabretta@st.com)

ABSTRACT Solder reliability is a key aspect for the packaging of low voltage power semiconductor device. The interconnections among package components, e.g. the silicon chip and copper leadframe, and between package itself and the external printed control board (PCB) should be properly designed to ensure the automotive durability requirements. In this framework, the proposed paper introduces an experimental-numeric characterization flow with the purpose to analyze solder visco-plasticity and fatigue during passive temperature cycle. The presented methodology has included solder mechanical characterization aimed to determine the parameters of Anand model which reproduces the solder visco-plastic behavior and the mechanical properties' temperature dependency. Finite element model has been employed to calculate the inelastic work which solder dissipates during each temperature cycle. Simulation results serve as input to predict solder lifetime according to an energetic method. Moreover, failure analyses have been performed to assess the failure mechanism and to check model correlation in terms of number of cycles to failure forecast.

INDEX TERMS Reliability, material characterization, finite element model, power semiconductor package.

I. INTRODUCTION

The diffusion of low voltage power devices is nowadays increasing in several applications such as mild-hybrid powertrains with bus voltage of 48 V. The state-of-art of mild hybrid systems acts for the battery charging, e.g. during braking phase, and for assisting the vehicle acceleration after Start&Stop. Nowadays this technology represents an entry level for car electrification while full-hybrid and full-electric solutions are forecast for the next future as the main target for car manufactures. Due to this current trend, the reliability of low voltage power device represents a crucial point. In the electronics industry, power device packages' durability is typically limited by the integrity of its interconnections. They ensure the electrical and mechanical links between the semiconductor chip, commonly named die, and the metallic leadframe inside the semiconductor packaging. Moreover, interconnections made by solder brazing are also employed to joint the entire power package with an heatsink or the external printed circuit board (PCB) in order to improve the thermal performances and to guarantee the electronic control.

The associate editor coordinating the review of this manuscript and approving it for publication was Hamid Mohammad-Sedighi.

The term *solder* defines a group of metal alloys, mainly tin-based, with a relative low melting temperature. Its working principle consists of the intermetallic (IMC) formation between the solder compound and the metallic parts to be brazed with. During an industrial soldering process, the alloy is melted, e.g. using a reflow vapor phase oven, then it is cooled down. IMCs are formed at the interfaces due to high diffusion enhanced by liquid phase. The solder microstructure and its mechanical properties are strongly affected by the temperature profile of the soldering process [1].

Thermo-mechanical modelling represents a useful tool for the structural assessment and the reliability optimization of solder interconnections [2]. Considering that solder works at high homologous temperature (from 0.45 T_m to 0.9 T_m) a viscous behavior has to be accounted. Moreover, due to the thermal stress induced on solder by temperature variation and mismatch of coefficient of thermal expansion (CTE), non-linear visco-plastic behavior may be considered for a proper solder modelling. According to literature, solder constitutive equation ranges from elasto-plastic models based on empirical stress-strain curves [3] to a pure creep models applied on time-dependent data [4]. In addition, there have

been proposed phenomenological models in which creep and plasticity have been fictitiously separated [5]. From the continuum mechanical stand-point, dislocation motion is the driving mechanism to describe both the time-dependent (creep) and time-independent (plasticity) inelastic strains. An unified material model is indeed suggested, resulting a valid and common approach for solder mechanical modeling [6]. In this framework, the most used method is the Anand model. It does not need an explicit yield condition and loading/unloading criterion. Moreover, the Anand's mathematical formulation employs an internal scalar variable s which correlates the averaged isotropic deformation resistance with the macroscopic plastic flow. Temperature and strain rate sensitivity are accounted by such methodology, as well as the history effects of temperature and strain rate, strain hardening, and also dynamic recovery [7]. The parameters of Anand model can be extrapolated deriving the formulation for the 1D case and employing uni-axial stress-strain test, as later shown in section II-B1. Parameters for Anand modeling may be extracted also by creep data, obtaining in both cases similar parameters' sets [8].

As previously mentioned, interconnection reliability is a key parameter to design and optimize a power package [9]. Devices are submitted in application conditions to periodic thermal profiles which are generated by device self-heating or by the variation of the environmental temperature. This produces fluctuating stresses and strains which generate solder's mechanical fatigue. A reliable lifetime estimation is needed to optimize the package design as function of costumer mission profile. The current models for thermal fatigue prediction might be classified in three macro-groups: strain-based, damage-based and energy-based models. The strain-based fatigue class predicts the number of cycle to failure starting from the cumulated inelastic strain for each cycle, typically calculated by finite element analysis (FEA). An example is Coffin-Manson equation. The main issue of such modeling approaches is the difficulty to distinguish the creep and plasticity phenomenology. According to this, strain-based models could be split in two subgroups which are creep and plasticity based-methods [10]. The damage-based fatigue models calculate the accumulated damage caused by crack propagation accounting on fracture mechanics theory, for example based on cohesive zone approach [11], [12]. The main drawback of damage-based fatigue model is the request for challenging FEA model and experimental characterization on dedicated prepared samples, e.g. double cantilever beam test [13], to characterize crack initiation and propagation as function of fracture mode-mixity. The energy-based models are the most diffused [10] and base the fatigue prediction on the calculation of the overall stress-strain hysteresis energy of solder compound. Two representative methodologies are the Pang *et al.* [14] and Darveaux [15] approaches. The dissipated energy is calculated by FEA and lifetime solder prediction can be forecast once model calibration with experimental reliability test on the same solder compound or according to literature results [16].

This paper proposes an integrated approach to characterize and assess the solder joint reliability of low voltage power devices as described in section II-A. Experimental uniaxial tensile tests have been carried out to determine the Anand constitutive model for the solder. The theoretical framework has been presented in section II-B1, the proposed design of experiments in section II-B2 and the results have been shown in section III-A. A dedicated FEA has been developed to calculate the hysteretic energy as explained in section II-C. Energy-based model (section II-D) has been considered for the lifetime estimation in a passive temperature cycle, as reported in section 5. Experimental reliability tests and failure analyses explained in section II-E have been employed to characterize the failure mechanisms, as depicted in section III-B. Finally, the numerical results and failure analyses have been compared in section IV.

II. MATERIALS AND METHOD

A. TEST VEHICLES AND EXPERIMENTAL TEST

An automotive low voltage power discrete packages has been accounted for the proposed reliability assessment. In this framework, the durability performance has been evaluated for passive temperature cycle test [17]. This trial consists of placing the devices under test (DUTs) in a climatic room which is able to control the temperature according to a specified cycle. The test target is to determine the capability of solder interconnections to withstand thermal stresses induced by the variation from high to low temperature extremes. The main activated failure mechanism is the solder delamination due to inelastic strain cumulated during the temperature cycling. Thermal stress has been applied considering packages soldered on test board. In this analysis, it has been considered a PCB with a thickness of 1.6 mm and with four copper layers of 70 µm. Optical images of power package and PCB is shown in fig. 1 together to a simplified cross-section of the entire system. referring to cross section, the silicon chip (typically named die) is soldered on a copper leadframe and a copper clip using PbSnAg solder, then it is encapsulated by epoxy molding compound in order to protect the chip from external environment (e.g., from humidity). Both processes require a thermal budget, therefore mechanical stress due to materials' CTE mismatch are induced by temperature variation during assembly flow. Then, power packages are soldered on PCB using Sn96Ag3.0Cu0.5 (SAC 305) alloy.

B. MATERIAL CHARACTERIZATION

1) THEORETICAL FRAMEWORK

As mentioned in the introduction, Anand material model is the most appropriate to describe solder mechanical behavior. Its constitutive equation is defined by nine material parameters and by scalar state variable s that represents the material resistance to the plastic flow. A typical expression of Anand model is given correlating the inelastic strain rate $\dot{\varepsilon}_p$ as follows:

$$\dot{\varepsilon}_p = A \exp\left(\frac{Q}{RT}\right)\left[\sinh\left(\xi\frac{\sigma}{s}\right)\right]^{1/m} \quad (1)$$

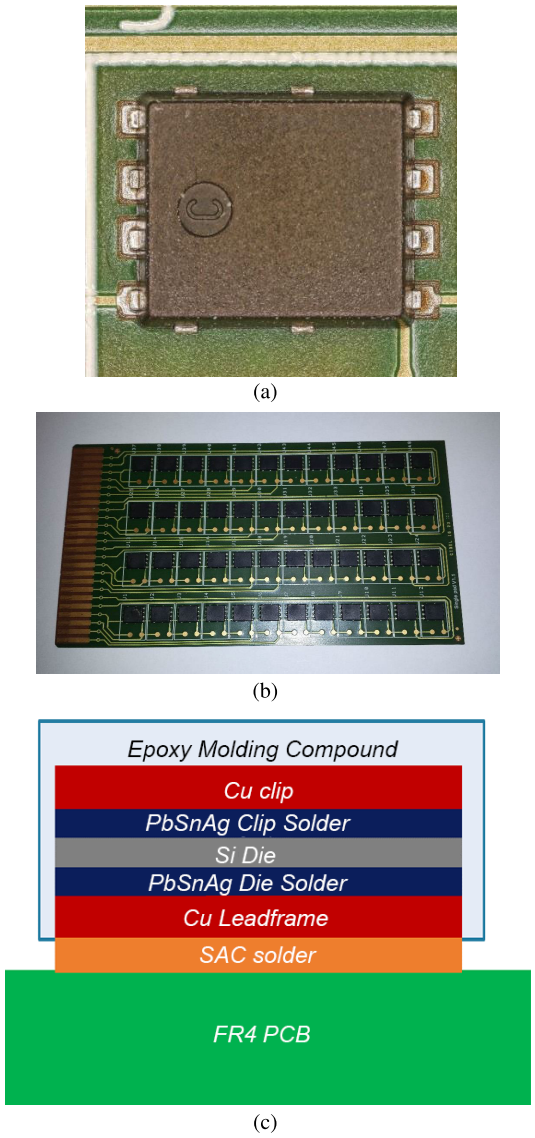

FIGURE 1. Optical images of power package stand-alone (a) and soldered on PCB (b). Moreover, a schematic cross section has been shown (c).

in which A is the pre-exponential factor, Q the activation energy, R the gas constant, T the absolute temperature, ξ the multiplier of stress, σ the equivalent Von Mises stress and m the strain rate sensitivity. The internal state variable s is included as a ratio with the equivalent stress, a typical Arrhenius relation is considered for the temperature dependence and the time dependency is accounted according to the hyperbolic sine form introduced by Ramachandran *et al.* [18] for the secondary creep. The state variable derivative $\dot{s}$ can be explicated as function of the strain hardening function h and of the saturation value of deformation resistance $s*$:

$$\dot{s} = h(\sigma, s, T)\,\dot{\varepsilon}_p = \left[h_0 \cdot \left|1 - \frac{s}{s^*}\right|^a \cdot \operatorname{sgn}\left(1 - \frac{s}{s^*}\right)\right]\dot{\varepsilon}_p \quad (2)$$

$$s^* = \hat{s}\left[\frac{\dot{\varepsilon}_p}{A}\exp\left(\frac{Q}{RT}\right)\right]^n \quad (3)$$

where h_0 is the hardening constant, a is the strain rate sensitivity of hardening, $\hat{s}$ is saturation coefficient and n is the strain rate sensitivity for the saturation value of deformation resistance. According to equations (1)-(3) all the nine material parameters have been defined as resumed in table 1.

TABLE 1. Material parameters for Anand model.

Symbol	Description	Measurement unit
A	pre-exponential factor	s^{-1}
Q/R	Arrhenius term	K
$\hat{s}$	saturation coefficient	MPa
ξ	multiplier of stress	dimensionless
m	strain rate sensitivity	dimensionless
h_0	hardening constant	MPa
s_0	deformation resistance initial value	MPa
n	strain rate sensitivity of saturation	dimensionless
a	strain rate sensitivity of hardening	dimensionless

Anand model can be extrapolated for one dimensional case [8]. Considering uniaxial stress condition, stress σ and internal state variable s can be correlated by a power law as shown below:

$$\sigma = c \cdot s = \frac{1}{\xi}\sinh^{-1}\left[\left(\frac{\dot{\varepsilon}_p}{A}\exp\left(\frac{Q}{RT}\right)\right)^m\right] \cdot s \quad (4)$$

in which the term c is lesser than 1. Arranging the above equations is possible to express the stress σ as function of strain ε and strain rate $\dot{\varepsilon}$:

$$\begin{aligned}\sigma &= \frac{1}{\xi}\sinh^{-1}\left[\frac{\dot{\varepsilon}_p}{A}\exp\left(\frac{Q}{RT}\right)\right]^m \cdot \\ &\cdot\left(\hat{s}\left[\frac{\dot{\varepsilon}_p}{A}\exp\left(\frac{Q}{RT}\right)\right]^n - \left\{\left[\hat{s}\left[\frac{\dot{\varepsilon}_p}{A}\exp\left(\frac{Q}{RT}\right)\right]^n - s_0\right]^{(1-a)}\right.\right. \\ &\left.\left. + (a-1)\left[h_0\left(\hat{s}\left[\frac{\dot{\varepsilon}_p}{A}\exp\left(\frac{Q}{RT}\right)\right]^n\right)^{-a}\right]\varepsilon_p\right\}^{\frac{1}{1-a}}\right) \quad (5)\end{aligned}$$

Due to the fact that uniaxial stress trials are performed at constant temperature T and at fixed strain rate $\dot{\varepsilon}_p$, the ultimate tensile strength (σ^*) can be found considering that plastic strain ε_p goes to ∞:

$$\sigma^* = \frac{\hat{s}}{\xi}\left[\frac{\dot{\varepsilon}_p}{A}\exp\left(\frac{Q}{RT}\right)\right]^n \cdot \sinh^{-1}\left[\frac{\dot{\varepsilon}_p}{A}\exp\left(\frac{Q}{RT}\right)\right]^m \quad (6)$$

Replacing the saturation stress in eq. (5) with the expression found in eq. (6), the post yield stress-strain response is expressed as:

$$\begin{aligned}\sigma = \sigma^* - \left\{\left(\sigma^* - c\,s_0\right)^{(1-a)} + \right. \\ \left. + (a-1)\left[(c\,h_0)\left(\sigma^*\right)^{-a}\right]\varepsilon_p\right\}^{1/(1-a)} \quad (7)\end{aligned}$$

By these equations' set, the nine parameters of Anand model resumed in table 1 can be determined by uniaxial stress-strain trials performed at different temperature and strain rate. By such tests it is possible to measure the saturation stress and the stress-strain relation during the plastic regime. The procedure for compiling the parameters of Anand model is made by two step. The six Anand parameters $\hat{s}$, ξ, A, Q/R, n and m are found by a nonlinear least-squares

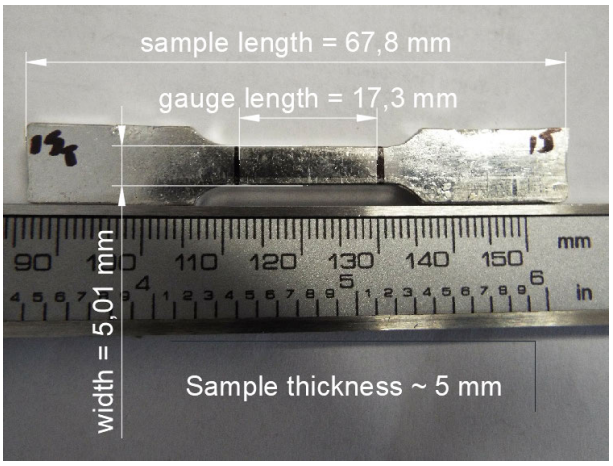

FIGURE 2. SAC 305 dogbone sample realized for uniaxial tensile test.

regression fit of eq. (6), considering the saturation stress recorded at different temperature and strain rate conditions. The other Anand parameters (s_0, h_0 and a) are determined starting from the experimental stress-strain data at some test conditions and fitting the parameters of eq. (7).

2) EXPERIMENTAL UNIAXIAL TENSILE TEST

Uniaxial stress-strain tests at different temperature and strain rate have been employed for the two analyzed solder compounds: PbSnAg alloy for die attach and SAC305 for package mounting on PCB. A total of twelve conditions have been accounted considering temperature and strain rate combination. Four temperature T values have been -40, 25, 75 and 125 °C, whereas the three considered strain rate $\dot{\varepsilon_p}$ have been 0.001, 0.0001 and 0.000 01 s^{-1}. Three samples has been considered for each strain rate/temperature combination (total of 36 samples). Solder samples have been caste in a dogbone mold according to the temperature reflow profile which is considered during industrial soldering process. Flat samples have been produced for both analyzed solder alloys with a width and thickness of 5 mm and gauge length of 17 mm, as shown in fig. 2.

C. FINITE ELEMENT MODEL

A nonlinear finite element analysis has been developed to calculate the dissipated energy in solder layers during a passive temperature cycle between -40 and 125 °C. Anand formulation has been included to reproduce solder visco-plasticity considering the experimental characterized parameters. Elastic behavior is assumed for the other materials. The linear mechanical material properties have been reported in table 2. For what concerns the properties of molding resin, it has been assumed resin glass transition does not occur during temperature cycle due to the fact the maximum cycle temperature (125 °C) is below the specific glass transition point (135 °C). Young modulus for PbSnAg and SnAgCu solders has been considered as function of temperature, according to equations (11) and (12) later presented.

The modeled geometry has been plotted in fig. 3. The three different package copper supports (leadframe, source clip lead and gate lead) have been described in this picture. As later shown, the cumulated fatigue depends on the specific solder joint between package and PCB. The geometry has been discretized by a prevalent hexahedral linear mesh (solid 187), as depicted in fig. 4. Mechanical boundary conditions have been set considering that the board is rested on a support plane and it is free to expand without mechanical constrains.

In order to properly calculate the visco-plastic work in solder compounds, it is needed to consider the mechanical stress on solder induced from the ''hot'' assembly process as described in section II-A. Dedicated model, with the proper temperature profile, has been built for each process step

TABLE 2. Material properties considered for mechanical FE simulation.

Material	Young Modulus [GPa]	CTE [ppm/K]	Poisson ratio
FR4	22	18	0.28
Copper	120	17.5	0.343
PbSnAg	Eq. (11)	30	0.35
SAC305	Eq. (12)	23	0.35
Silicon	120	2.5	0.22
Resin	25	10	0.34

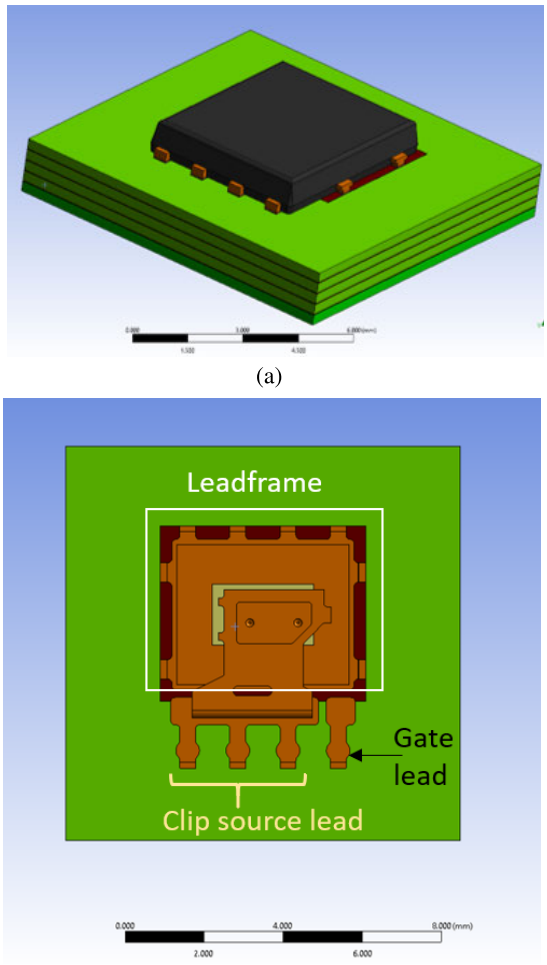

FIGURE 3. Isometric view of entire simulated stack (a) and top view without molding case (b) in which the three different package supports (leadframe, source clip lead and gate lead) have been distinguished.

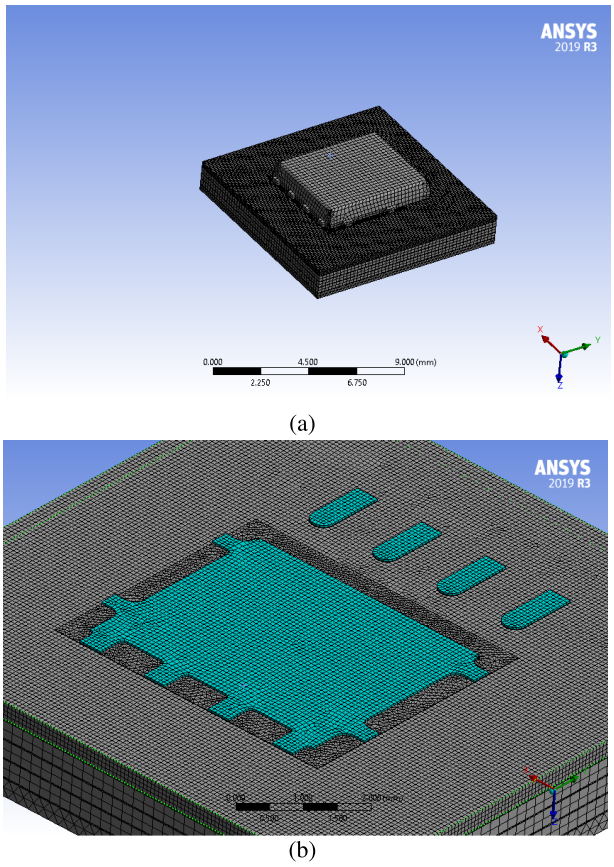

FIGURE 4. Meshed geometry, with a complete view (a) and a detail on SAC layers (b).

TABLE 3. Darveaux parameters for PbSnAg [16] and SAC 305 [19].

Parameters	Unit measurement	PbSnAg	SAC 305
K_1	$[cycles/MPa^{K_2}]$	11.6	37.97
K_2	[-]	-1.52	-2.8
K_3	$[mm/(cycles \cdot MPa^{K_2}]$	1.95e-3	1.4e-3
K_4	[-]	0.98	1.16

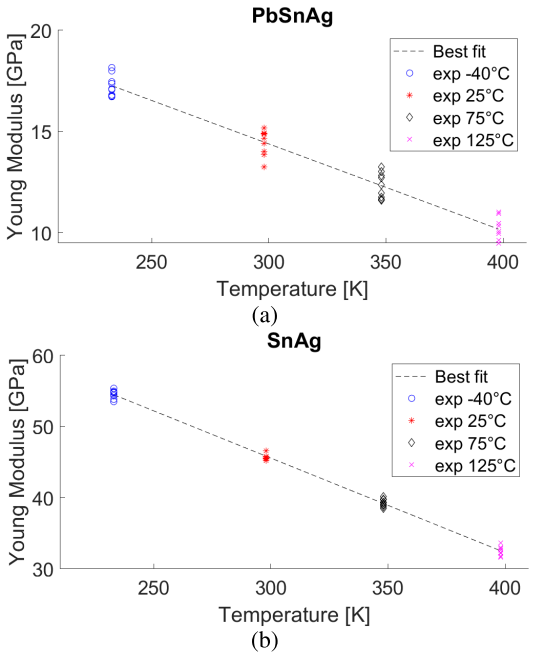

FIGURE 5. Data fitting for Young modulus vs temperature for PbSnAg (a) and SAC305 (b).

(die attach, molding and package soldering on PCB). In order to include or exclude the materials in the different model (e.g., during die attach process there is already not resin), the not-real layer are deactivated using a very low elastic modulus. In this way, these deactivate elements do not contribute to the FEA stiffness matrix; on the other side deformation continuity is guaranteed and they can be activated in the step in which they are introduced. Finally, temperature cycling has been simulated. In order to have a repetitive dissipation energy in two consecutive thermal cycles, several cycles have been simulated.

D. FATIGUE ANALYSIS

The Darveaux's energetic approach [15] has been selected to predict the reliability behavior of solder joints. This method has established four empirical constants (K_1, K_2, K_3 and K_4) for each solder compound which correlate crack growth with visco-plastic energy and cycles to failure. Mathematical formulation has been reported below:

$$N_0 = K_1(\Delta W)^{K_2} \tag{8}$$

$$\frac{dl}{dN} = K_3(\Delta W)^{K_4} \tag{9}$$

in which N_0 is the number cycles of crack initiation, $\frac{dl}{dN}$ is the crack propagation rate and ΔW the average dissipated energy density in each solder layer during a complete temperature cycle. Starting from previous equations, the lifetime N_f can be expressed as:

$$N_f = N_0 + \frac{l_0}{K_3(\Delta W)^{K_4}} \tag{10}$$

in which l_0 is a characteristic dimension of the solder joint. In this framework, l_0 values have been selected equal to the solder length. The four parameters K_i have been chosen according to literature source: [16] for PbSnAg and [19] for SnAgCu as shown in table 3.

E. RELIABILITY STRESS AND FAILURE ANALYSIS

As mentioned in section II-A, packages assembled with SAC 305 on a 4-layer PCB have been submitted at a passive temperature between −40 and 125 °C in a dual-chambers environment in which thermal stress is induced transferring the DUTs from cold to the hot chamber and viceversa. Thermal cycle duration has been 30 minutes according to JESD22-A104F condition G,3 [17]. Dedicated optical analysis and scanning electron microscopy (SEM) have been performed to confirm the expected failure mode (solder delamination) and to benchmark model accuracy in terms of number of cycles to failure. Crack propagation has been characterized looking to cross section prepared by means of focus ion beam at several intermediate read-outs during the reliability stress.

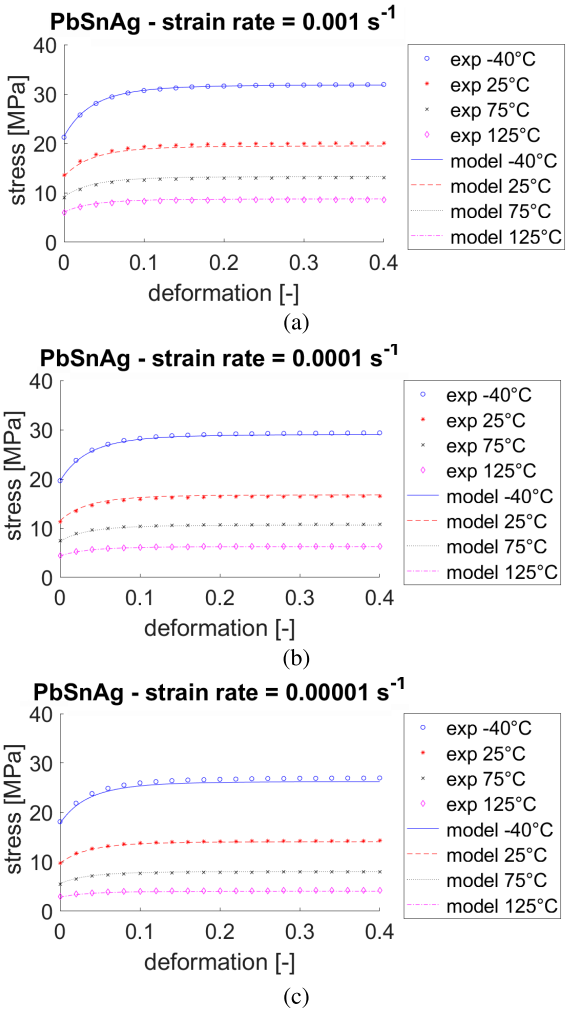

FIGURE 6. PbSnAg experimental (markers) and model (lines) plastic deformation-stress curves at different temperature, for the three analyzed strain rate: (a) 0.001 s^{-1}, (b) 0.0001 s^{-1} and (c) 0.00001 s^{-1}.

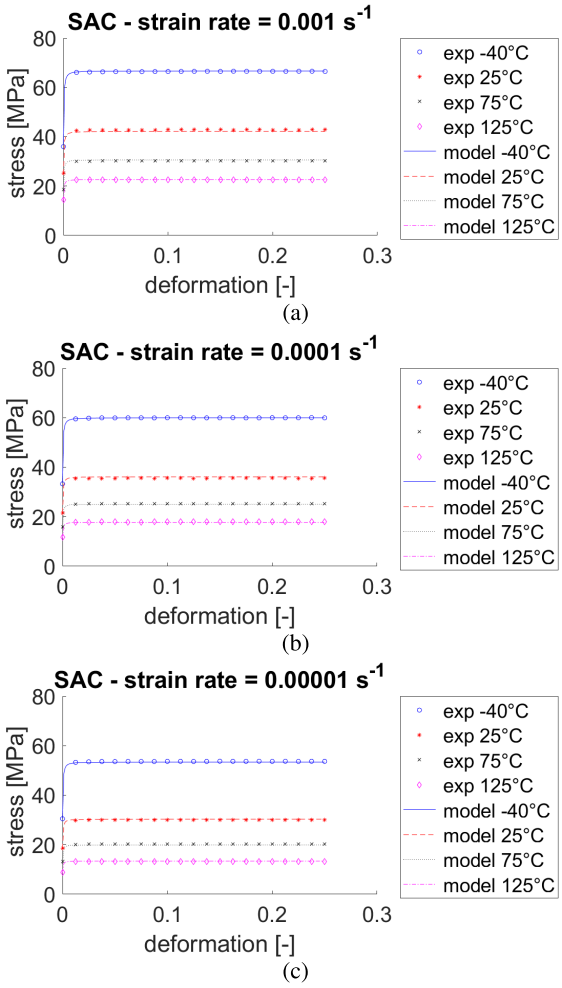

FIGURE 7. SnAgCu experimental (markers) and model (lines) plastic deformation-stress curves at different temperature, for the three analyzed strain rate: (a) 0.001 s^{-1}, (b) 0.0001 s^{-1} and (c) 0.00001 s^{-1}.

III. RESULTS

A. MATERIAL CHARACTERIZATION

Tensile tests at different temperature (−40, 25, 75 and 125 °C) and strain rate (0.001, 0.0001 and 0.000 01 s^{-1}) have been employed for the two solder alloy under test: PbSnAg and SAC 305. Young modulus has been determined as function of temperature, finding the linear relations:

$$E_{PbSnAg} = 27266 - 42.9\,T\ [MPa] \quad (11)$$

$$E_{SAC305} = 85267 - 128.5\,T\ [MPa] \quad (12)$$

Data regression is shown in fig. 5. It has been highlighted that SAC 305 has an higher Young modulus with respect to PbSnAg. Due to higher homologous temperature, SAC modulus present a higher sensitivity to temperature increasing.

According to the methodology explained in section II-B1, Anand parameters have been characterized for the solder compound under analysis. Fig. 6 shows the post-yield stress/strain curve for the PbSnAg alloy at different temperature and strain rate. The same output for SnAgCu alloy is reported in fig. 7. Experimental data are plotted together to the theoretical curves predicted with the experimental-predicted coefficients of Anand model which are reported in table 4. Optical microscopy has been performed on fractured parts after tensile test. Cup-cone fracture has been highlighted on dogbone samples as depicted in fig 8. This found is coherent with the characteristic ductile failure pattern which is typical of such kind of solder alloys.

TABLE 4. Measured Anad parameters for PbSnAg and SAC solders.

Parameter	PbSnAg	SAC 305
A	500,000	100,000
Q/R	1095.3	9320
$\hat{s}$	38.2	73.2947
ξ	9.48	5.09
m	0.28	0.16
h_0	1418.1	326,680
s_0	26.74	46.41
n	0.002	0.006
a	1.20	1.74

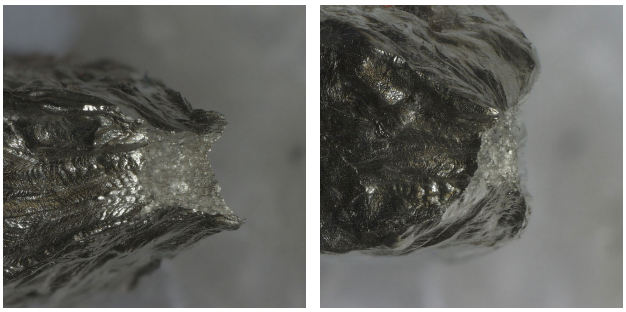

(a) (b)

FIGURE 8. Optical analysis on a failed SAC samples for uni-axial tensile test. It has been highlighted the cup (a) and cone (b) parts typical of the ductile fracture.

TABLE 5. Predicted number to cycle for crack initiation (N_0) and total lifetime (N_f) for package and PCB solder layer.

Layer	Compound	Inelastic work	N_0	N_f
Die attach	PbSnAg	0.05 MPa	1.1k	40k
Clip attach	PbSnAg	0.04 MPa	1.5k	50k
Source lead attach	SAC	0.18 MPa	4.6k	15k
Leadframe attach	SAC	0.16 MPa	6.4k	15k
Gate lead attach	SAC	0.21 MPa	3.0k	4.7k

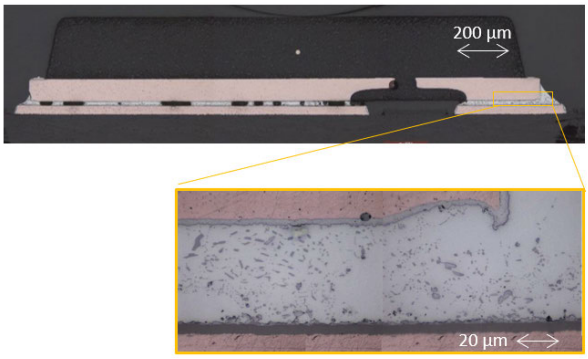

FIGURE 9. Optical analysis on cross-section before test starting. No cracks have been pointed out..

B. FE RESULTS AND FATIGUE ESTIMATION

The performed finite element simulation has highlighted that the most critical joint in terms of fatigue behavior has been the SAC solder between PCB and the gate lead, previously described in fig. 3. Simulation outcome is the inelastic work cumulated for each temperature cycle, then reliability prediction in terms of lifetime has been done according to procedure and equations shown in section II-D. According to the numerical outputs reported in table 5, the initial number of cycle for crack initiation in gate lead attach is around 3000 cycles while a massive failure has been predicted at around 4700 cycles. Crack initiation has been forecast at lower number of cycle N_0 for PbSnAg while total lifetime N_f is more extended for these interconnections. The explanation is related due to the fact that PbSnAg solder are wider than SAC joints, indeed a much longer crack length is needed to have a detrimental effect on device electrical and thermal characteristics.

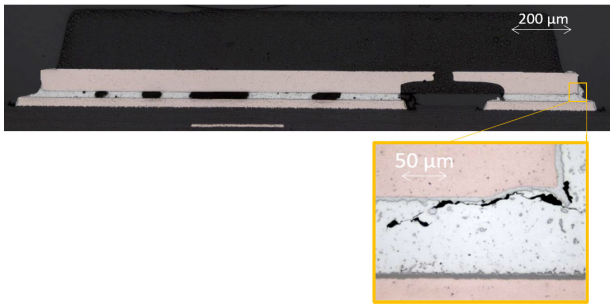

FIGURE 10. Optical analysis on cross-section after 3000 temperature cycles. Incipient crack has been pointed out in gate lead solder.

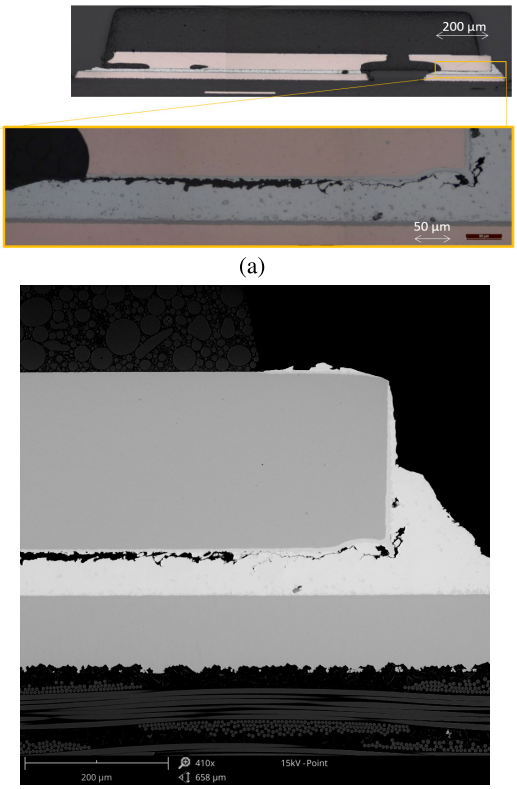

FIGURE 11. Optical analysis on cross-section after 5000 temperature cycles (a) and SEM with low magnification (b). Massive delamination between solder and gate lead has been detected.

C. EXPERIMENTAL ANALYSIS

Optical analysis has been performed on sample cross section which are executed at partial readout every 500 cycles. Analysis performed before test starting has not shown crack evidence in solder layer, as reported in fig. 9.

The microscopy investigation done after 3000 cycles (fig. 10) shows the crack initiation in the interface between gate lead solder and package. Optical analysis performed after 5000 cycles has reported a complete failure of this solder joint. As also confirmed by SEM, SAC-gate lead interface result totally delaminated (fig. 11).

IV. DISCUSSION AND CONCLUSION

Tensile characterization of solder alloys reported in section III-A has shown SAC behaves with higher stiffness than PbSnAg, leading to the different Anand parameters as shown in table 4. These Anand constitutive equations has been the input of simulation model for passive temperature cycling reliability stress. The inelastic work cumulated in each stress cycle has been calculated by finite element analysis, as reported in section III-B and resumed in table 5. Dissipated energy is higher in PbSnAg (die and clip attach inside the package) than in SAC board-level solders. Nevertheless, according to the narrow dimensions of joints between package supports and PCB, SAC interconnections have been predicted as the most critical during the reliability stress. The joint between gate lead and test board results as the most stressed part by passive thermal swing and, due to Darveaux fatigue formulation, it has been forecast that crack initiates at 3000 cycles and total delamination occurs at 4700 cycles. As mentioned in section III-C, the failure analysis on dedicated samples extracted at partial read-out has supported the numerical prediction, highlighting also that delamination involves specifically the interface between solder and package copper lead.

In this paper it has been presented a complete characterization flow to analyze package and board level solder reliability, starting from experimental solder material assessment and ending with method validation by comparison between numerical prediction and failure analysis results. The confirmed model calibration allows to predict just by model the effect of design option in terms of geometry or bill of materials, e.g. the mechanical impact of a top side cooling solution or, in the framework of pollution reduction, the replacement of lead based alloy with SAC. The proposed model and energy-based fatigue formulation can be extended also to other kind of reliability test, such as active power cycling which is closer to application conditions than passive temperature cycling. Furthermore, the proposed methodology could be extended for the characterization of novel power electronic interconnection materials, e.g. silver sintering or hybrid glues.

REFERENCES

[1] M. M. Basit, M. Motalab, J. C. Suhling, and P. Lall, "The effects of aging on the anand viscoplastic constitutive model for SAC305 solder," in *Proc. 14th Intersoc. Conf. Thermal Thermomech. Phenomena Electron. Syst. (ITherm)*, May 2014, pp. 112–126.

[2] J. Wilde, K. Becker, M. Thoben, W. Blum, T. Jupitz, G. Wang, and Z. N. Cheng, "Rate dependent constitutive relations based on Anand model for 92.5Pb5Sn2.5Ag solder," *IEEE Trans. Adv. Packag.*, vol. 23, no. 3, pp. 408–414, Aug. 2000.

[3] A. Morozumi, H. Hokazono, Y. Nishimura, E. Mochizuki, and Y. Takahashi, "Influence of antimony on reliability of solder joints using sn-sb binary alloy for power semiconductor modules," *Trans. Jpn. Inst. Electron. Packag.*, vol. 8, no. 1, pp. 8–17, 2015.

[4] A. Sitta, M. Calabretta, M. Renna, and D. Cavallaro, "Solder joint reliability: Thermo-mechanical analysis on power flat packages," in *Advances on Mechanics, Design Engineering and Manufacturing* (Lecture Notes in Mechanical Engineering), B. Eynard, V. Nigrelli S. Oliveri, G. Peris-Fajarnes, and S. Rizzuti, Eds. Cham, Switzerland: Springer, 2017, doi: 10.1007/978-3-319-45781-9_71.

[5] Y. Pao, S. Badgley, E. Jih, R. Govila, and J. Browning, "Constitutive behavior and low cycle thermal fatigue of 97Sn-3Cu solder joints," *ASME J. Electron. Packag.*, vol. 115, no. 2, pp. 147–152, Jun. 1993, doi: 10.1115/1.2909310.

[6] C. Durand, M. Klingler, D. Coutellier, and H. Naceur, "Power cycling reliability of power module: A survey," *IEEE Trans. Device Mater. Rel.*, vol. 16, no. 1, pp. 80–97, Mar. 2016.

[7] G. Chen, X. Zhao, and H. Wu, "A critical review of constitutive models for solders in electronic packaging," *Adv. Mech. Eng.*, vol. 9, no. 8, 2017, Art. no. 1687814017714976.

[8] M. Motalab, Z. Cai, J. C. Suhling, and P. Lall, "Determination of anand constants for SAC solders using stress-strain or creep data," in *Proc. 13th Intersoc. Conf. Thermal Thermomech. Phenomena Electron. Syst.*, May 2012, pp. 910–922.

[9] M. Calabretta, A. Sitta, S. M. Oliveri, and G. Sequenzia, "Design and process optimization of a sintered joint for power electronics automotive applications," in *Design Tools and Methods in Industrial Engineering* (Lecture Notes in Mechanical Engineering), C. Rizzi, A. Andrisano, F. Leali, F. Gherardini, F. Pini, and A. Vergnano, Eds. Cham, Switzerland: Springer, 2020, doi: 10.1007/978-3-030-31154-4_40.

[10] W. W. Lee, L. T. Nguyen, and G. S. Selvaduray, "Solder joint fatigue models: Review and applicability to chip scale packages," *Microelectron. Rel.*, vol. 40, no. 2, pp. 231–244, Feb. 2000.

[11] R. Dudek, R. Pufall, B. Seiler, and B. Michel, "Studies on the reliability of power packages based on strength and fracture criteria," in *Proc. 12th Int. Conf. Thermal, Mech. Multi-Phys. Simulation Experiments Microelectron. Microsyst.*, Apr. 2011, pp. 1–8.

[12] A. Abdul-Baqi, P. J. G. Schreurs, and M. G. D. Geers, "Fatigue damage modeling in solder interconnects using a cohesive zone approach," *Int. J. Solids Struct.*, vol. 42, nos. 3–4, pp. 927–942, Feb. 2005.

[13] W. E. R. Krieger, S. Raghavan, and S. K. Sitaraman, "Experiments for obtaining cohesive-zone parameters for copper-mold compound interfacial delamination," *IEEE Trans. Compon., Packag., Manuf. Technol.*, vol. 6, no. 9, pp. 1389–1398, Sep. 2016.

[14] J. H. L. Pang, B. S. Xiong, and T. H. Low, "Creep and fatigue characterization of lead free 95.5Sn-3.8Ag-0.7Cu solder," in *Proc. 54th Electron. Compon. Technol. Conf.*, vol. 2, Jun. 2004, pp. 1333–1337.

[15] R. Darveaux, "Effect of simulation methodology on solder joint crack growth correlation," in *Proc. 50th Electron. Compon. Technol. Conf.*, May 2000, pp. 1048–1058.

[16] X. Xie, X. Bi, and G. Li, "Thermal-mechanical fatigue reliability of pbsnag solder layer of die attachment for power electronic devices," in *Proc. Int. Conf. Electron. Packag. Technol. High Density Packag.*, Aug. 2009, pp. 1181–1185.

[17] *Temperature Cycling*, JEDEC Solid State Technology Association Standard JESD22-A104F, 2020.

[18] V. Ramachandran, K. C. Wu, and K. N. Chiang, "Overview study of solder joint reliablity due to creep deformation," *J. Mech.*, vol. 34, no. 5, pp. 637–643, Oct. 2018.

[19] M. Motalab, M. Mustafa, J. C. Suhling, J. Zhang, J. Evans, M. J. Bozack, and P. Lall, "Correlation of reliability models including aging effects with thermal cycling reliability data," in *Proc. IEEE 63rd Electron. Compon. Technol. Conf.*, May 2013, pp. 986–1004.

MICHELE CALABRETTA received the M.S. degree in mechanical engineering and the Ph.D. degree in mathematics applied to engineering from the University of Catania, Catania, Italy, in 2005 and 2009, respectively.

From 2005 to 2008, he was a Research and Development Engineer with Ferrari S.p.A, Maranello, Italy. From 2008 to 2011, he was a Simulation Team Leader with Automobili Lamborghini, Sant'Agata Bolognese, Italy. He has been involved in design and multi-physics simulation (CAD/CAE) and material characterization. Since 2011, he has been with STMicroelectronics, Catania, where he is currently an Advanced Simulation and Characterization Manager with the Automotive and Discrete Group (ADG), Research and Development Department. His research interests include semiconductor packaging and reliability aspects, lifetime modeling, and multi-physics simulations.

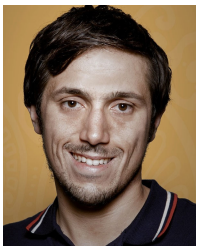

ALESSANDRO SITTA received the M.S. degree in mechanical engineering and the Ph.D. degree in system, energetic, computer and telecommunication engineering from the University of Catania, Italy, in 2016 and 2021, respectively.

Since 2017, he has been a Research Engineer with the Automotive and Discrete Group, Research and Development Department, STMicroelectronics, Catania, Italy. His research interests include power semiconductor device thermo-mechanical modeling, reliability estimation, and material and device experimental characterization.

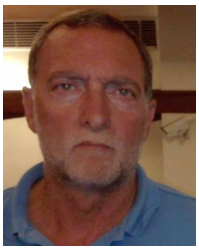

SALVATORE MASSIMO OLIVERI received the M.S. degree in engineering from the University of Catania, Catania, Italy, in 1977.

From 1990 to 1998, he was Research Assistant with the Machine Construction Group, University of Catania. From 1998 to 2005, he was an Associate Professor with La Sapienza University, Rome, Italy. Since 2005, he has been a Full Professor of design and method of the industrial engineering with the Department of Electric, Electronic and Informatic Engineering, University of Catania. He has developed, in the course of his academic career, scientific activities in different fields of the machine design that get from strain and stress analysis, to CAD in mechanical design, to fatigue in welds, to study of complex kinematics using multi-body software. He has managed and cooperated to the research activity with some Italian University, C.R.F. in Orbassano and ELASIS in Pomigliano d'Arco, and some Italian industries, such as Ferrari S.p.A., Ducati Motors Holding S.p.A., Fiat Auto, and Piaggio V.E. S.p.A.).

GAETANO SEQUENZIA received the M.S. degree in mechanical engineering and the Ph.D. degree in mathematics applied to engineering from the University of Catania, Catania, Italy, in 2004 and 2008, respectively.

Since 2008, he has been a Researcher with the Department of Electric, Electronic and Informatic Engineering (DIEEI), University of Catania. His research interests include strain and stress analysis, multibody dynamics, reverse engineering, and rapid prototyping.

Dr. Sequenzia is a member of ADM, the Italian Association of Design and Methods of the Industrial Engineering. His research activity is documented by numerous lectures and articles.